# Multi-UAV Cooperative Smoke-Screen Obscuration Strategy Based on LOS Geometric Occlusion Evaluation and PSO

Fuliang Xu, Liangwei Guo *

Xi'an University of Architecture and Technology, Xi'an, China

* Corresponding Author Email: 2845459422@qq.com

**Abstract.** This paper addresses smoke screen occlusion protection tasks in multi-missile attack scenarios by establishing a universal solution framework that integrates geometric determination with intelligent optimization. First, motion models are developed for missiles, UAVs, and smoke grenades, abstracting targets as cylinders and describing missile observation paths via discretized line-of-sight (LOS) segments. Subsequently, an occlusion criterion based on the minimum distance between LOS segments and spherical smoke clouds is proposed, and the effective duration is computed via time discretization with boundary refinement. Under coordinated multiple smoke grenade conditions, the occlusion region is further modeled as the union of multiple spherical smoke clouds, and strategy optimization is achieved by maximizing cumulative occlusion time. For multi-target scaling, a Max-Min robust fairness objective is introduced to ensure stable performance of the protection strategy even under the most unfavorable attack direction. Finally, a Particle Swarm Optimization (PSO) algorithm is employed for global search of mixed continuous-discrete variables, with a feasibility repair mechanism designed to guarantee constraint satisfaction.

**Keywords:** Particle Swarm Optimization, Multi-UAV Cooperative Optimization, Robust Fairness Optimization.

## 1. Introduction

In modern complex adversarial environments, incoming missiles often feature high-speed maneuvering and autonomous guidance, making hard-kill interception costly, time-critical, and difficult to scale for multi-target engagements. Soft protection using smoke screens to disrupt the seeker's line-of-sight (LOS) is attractive for its flexible deployment and low resource demand. Yet in multi-missile approach scenarios, smoke-grenade release timing, detonation position, and UAV trajectory planning are strongly coupled. Existing approaches often rely on simplified criteria or local search, leading to limited fidelity and suboptimal solutions [1] [2]. To address this, this paper proposes a general algorithmic framework for multi-platform cooperative smoke shielding: unified kinematic modeling of missiles, UAVs, and smoke grenades; a computable obscuration metric by converting shielding judgment into distance constraints between LOS segments and spherical smoke clouds; union-based modeling of multiple smoke regions with full-time-domain cumulative obscuration duration for fine-grained effectiveness quantification [3]. For multi-missile defense, a Max–Min robust objective is introduced to improve worst-case fairness, and particle swarm optimization is employed to globally solve the resulting mixed-variable problem [4]. A representative UAV smoke deployment scenario demonstrates stable coordinated shielding strategies under physical constraints, offering a reusable modeling-and-solution paradigm for complex soft-defense tasks.

## 2. Geometric LOS Occlusion Modeling and Single-Smoke Simulation Solution

### 2.1. Model Formulation

A 3D Cartesian coordinate system is defined with the decoy target at the origin. The true target is modeled as a cylinder and discretized into representative surface points to construct LOS segments.

#### 2.1.1. Kinematic Model of Missile M1

Let the missile position at time $t$ be $M(t)\in\mathbb{R}^3$. The missile travels at a constant speed of 300 m/s toward the decoy target (the origin). The kinematic model is

$$M(t)=M(0)+300t\cdot d_m,\qquad d_m=-\frac{M(t)}{|M(t)|} \tag{1}$$

#### 2.1.2. Kinematic Model of the UAV

The UAV FY1 starts from $F_1(0)$ and moves at a constant speed $v_0$ along a straight line at constant altitude, heading toward the decoy target. The motion equation is

$$F_1(t)=F_1(0)+v_0t \tag{2}$$

#### 2.1.3. Kinematic Model of the Smoke Cloud

The canister detonates at time $t_b$ with detonation position $C_b=P(t_b)$. A spherical smoke cloud with effective radius $R_s$ is formed instantaneously. The cloud center descends along the $-z$ direction at 3 m/s, and the effective obscuration duration is 20 s. The cloud center is modeled as

$$C(t)=C_b+(0,0,-3)(t-t_b) \tag{3}$$

### 2.2. Determination of the Obscuration Criterion

#### 2.2.1. Definition of Line-of-Sight: Target Discretization and Single Line-of-Sight

To approximate surface visibility, the cylinder is discretized into 8 equally spaced azimuth angles $\theta_k$ on the horizontal plane. The sampled points on the bottom and top rims are

$$B_k=\left(R\cos\theta_k,\,200+R\sin\theta_k,\,0\right),\qquad T_k=\left(R\cos\theta_k,\,200+R\sin\theta_k,\,H\right) \tag{4}$$

The representative set is $\nu=\{B_0,\ldots,B_7,T_0,\ldots,T_7\}$. Given missile position $M(t)$ and any $X\in\nu$, the LOS segment is defined as $\overline{M(t)X}=\{M(t)+s(X-M(t))|\ s\in[0,1]\}$.

#### 2.2.2. Definition of the Smoke Cloud

For $t\in[t_b,t_b+20]$, the smoke cloud is modeled as a sphere centered at $C(t)$ with radius $R_s$:

$$\mathbb{B}(C(t),R_s)=\{x\in\mathbb{R}^3||x-C(t)|\le R_s\} \tag{5}$$

At time $t$, the LOS to a point $X\in\nu$ is considered obscured if the segment $\overline{M(t)X}$ intersects the ball $\mathbb{B}(C(t),R_s)$. This intersection test is equivalent to computing the minimum distance $D_X(t)$ from the cloud center to the segment. Obscuration holds if and only if $D_X(t)\le R_s$.

### 2.3. Implementation of Distance Calculation

#### 2.3.1. Distance from a Point to a Line Segment for a Single Line-of-Sight

For a given $X\in\nu$, define $u=X-M(t)$ and $w=C(t)-M(t)$. The projection parameter is

$$\lambda'=\frac{w\cdot u}{u\cdot u},\qquad \lambda=\min\{1,\max\{0,\lambda'\}\} \tag{6}$$

The closest point on the segment is $Q=M(t)+\lambda u$, and the minimum distance is

$$D_X(t)=|C(t)-Q|=|C(t)-(M(t)+\lambda(X-M(t)))| \tag{7}$$

#### 2.3.2. Time Discretization and Accumulation of Effective Duration

Time is discretized over $[t_b, t_b+20]$ with step size $\Delta t$. The value $\Delta_h(t_k)$ is evaluated sequentially. When adjacent time steps switch between "obscured" and "not obscured", bisection refinement is applied to localize the boundary time more accurately. The full-obscuration intervals are then accumulated to obtain the total effective duration.

## 3. Multi-Canister Parameterized Modeling and Grid Search Optimization

### 3.1. Model Formulation

#### 3.1.1. Problem Description and Modeling Objectives

The task is to optimize the UAV heading, speed, and the release/detonation schedule of three smoke canisters to maximize the full-obscuration duration under feasibility constraints.

#### 3.1.2. Decision Variables

The decision variables include the UAV heading $\phi$, UAV speed $v$, and the release/detonation times of three canisters: drop times: $t_{d,1}$, $t_{d,2}$, $t_{d,3}$; detonation times: $t_{b,1}$, $t_{b,2}$, $t_{b,3}$; The detonation time is defined by a fuse delay: $t_{b,i}=t_{d,i}+\tau_i$.

#### 3.1.3. Objective Function: Maximizing the Cumulative Obscuration Duration

Let $\mathcal{S}(t)$ denote the union of smoke clouds at time $t$. For each discretized LOS (represented by the target-point set $\nu$), an obscuration indicator is evaluated, and the time length satisfying full obscuration is accumulated as $T_{\text{cov}}$. The optimization objective is

$$\max T_{\text{cov}}(\phi, v, t_{d,1:3}, t_{b,1:3}) \tag{8}$$

#### 3.1.4. Constraints

1. Timing and Feasibility Constraints: To ensure implementability, an equally spaced drop schedule is enforced: $t_{d,1}\geq 0,\ \Delta\geq 1\text{s},\ t_{d,2}=t_{d,1}+\Delta,\ t_{d,3}=t_{d,1}+2\Delta$. Fuse delays satisfy: $\tau_i\geq 0,\ \tau_1=\tau_2=\tau_3=\tau$

2. Heading Angle Range: $-\pi\leq\phi<\pi$.

3. Speed Range / Discrete Gears: The speed range is $70\leq v\leq 140$, and the speed is selected from the discrete set $v\in\{70,80,90,100,110,120,130,140\}$ m/s.

4. Drop-Detonation Relationship: $t_{d,i}\geq 0,\ \tau_i\geq 0,\ t_{b,i}=t_{d,i}+\tau_i$.

5. Missile Kinematic Constraints: Missile trajectories must satisfy predefined kinematic equations.

6. UAV Kinematic Constraints: The UAV trajectory must follow the constant-speed, fixed-heading straight-line flight model.

7. Smoke Canister Ballistic Constraints: After being released from the UAV, smoke canisters are only subjected to gravity. Their trajectories satisfy the projectile motion model $P_i(t)$ before detonation.

8. Smoke Cloud Validity Constraints: Each smoke canister detonates at $t_{b,i}$ to form a cloud. The cloud center descends at 3 m/s, and the cloud is only effective within the time interval $[t_{b,i}, t_{b,i}+20]$.

9. Obscuration Criterion Constraints: For a discrete missile-target LOS segment $\overline{M(t)X}$ ($X\in\nu$), the LOS is deemed obscured if the minimum distance from the cloud center to the segment is no more than $R_s$. Full obscuration is determined if the condition is satisfied for all $X\in\nu$ simultaneously.

### 3.2. Model Solution

Step 1 Kinematics and Parameterization of Three-Canister Timing (Variable Reduction)

With the parameterization "shared fuse delay + equally spaced releases", the original timing variables can be reduced to six interpretable decision variables, which decreases the search complexity while preserving dominant factors.

1. Missile trajectory: With initial position $M(0)$, speed 300 m/s, and direction toward the $d_m$.

2. Ballistics and detonation of canister $i$: Upon release, the canister inherits the UAV horizontal velocity and is affected by gravity $g$ vertically. For $t \geq t_{d,i}$:

$$P_i(t) = F(t_{d,i}) + v(\cos\phi, \sin\phi, 0)(t - t_{d,i}) + \frac{1}{2}(0, 0, -g)(t - t_{d,i})^2 \tag{9}$$

Detonation time and position are $t_{b,i} = t_{d,i} + \tau_i, \quad C_{b,i} = P_i(t_{b,i})$.

The cloud center evolves as $C_i(t) = C_{b,i} + (0, 0, -3)(t - t_{b,i})$.

3. Six decision variables: Define the decision variable set is $(\phi, v, t_{d,1}, \tau_1, \Delta t_d, \Delta\tau)$, and derive the extended timing parameters:

$$t_{d,2} = t_{d,1} + \Delta t_d, \quad t_{d,3} = t_{d,1} + 2\Delta t_d, \quad \tau_2 = \tau_1 + \Delta\tau, \quad \tau_3 = \tau_1 + 2\Delta\tau, \quad t_{b,i} = t_{d,i} + \tau_i \tag{10}$$

Step 2 Geometric Definition of Multiple Smoke Clouds

The $i$-th active smoke cloud (within its valid time window) is modeled as a closed ball:

$$\mathbb{B}_i(t) = \{x \in \mathbb{R}^3 \mid |x - C_i(t)| \leq R_s\}, \quad t \in [t_{b,i}, t_{b,i} + 20] \tag{11}$$

The effective smoke-obscured region at time $t$ is the union of all active clouds:

$$\mathcal{S}(t) = \bigcup_{i=1}^{3} \mathbb{B}_i(t) \tag{12}$$

Step 3 Numerical Implementation of Cumulative Obscuration Duration

1. Single LOS vs. multiple spheres: For any discrete target point $X \in \nu$, define the minimum distance from the point to the union of smoke clouds:

$$d_{\min}(t; X) = \min_{i \in \{1,2,3\}} d\left(C_i(t), \overline{M(t)X}\right) \tag{13}$$

where $d(\cdot, \overline{M(t)X})$ denotes the minimum distance from a point to the LOS segment. The LOS to $X$ is obscured if $d_{\min}(t; X) \leq R_s$.

2. Full obscuration at a time instant: Define the worst-case minimum distance across all discrete target points:

$$z(t) = \max_{X \in \nu} d_{\min}(t; X) \tag{14}$$

Full obscuration (all 16 LOS segments blocked) holds when $z(t) \leq R_s$.

3. Full-time cumulative duration

Discretize time samples $t_k$ over the union of valid time windows of the three clouds, and compute $z(t_k)$ for each sample. Bisection refinement is applied around state transitions (obscured ↔ non-obscured) to obtain precise critical times. The total effective obscuration duration is the sum of lengths of disjoint fully obscured intervals $T_{\text{cov}} = \sum_m (e_m - s_m)$, where $s_m$ and $e_m$ are the start/end times of the $m$-th fully obscured interval.

Step 4 Variable Discretization and Grid Search

Grid-search discretization uses the following step sizes (to balance accuracy and computational cost): Heading angle $\phi$: $[-\pi, \pi]$ with a step of $10^{\circ}$; UAV speed $v$: $[70,140]$ m/s with a step of 10 m/s; Time variables ($t_{d,1}$, $\tau$, $\Delta t_d$, $\Delta\tau$): step of 0.1 s.

Feasibility Constraints: Smoke-related time variables are upper-bounded by 4 s to satisfy mission timing constraints; grid points exceeding this upper bound are marked as infeasible and discarded.

For each feasible grid point:

1. Use Step 1 to derive all release/detonation times ($t_{d,i}$, $t_{b,i}$) and cloud trajectories $C_i(t)$;
2. Use Step 3 to compute the total effective obscuration duration $T_{\text{cov}}$;
3. Select the grid point with the maximum $T_{\text{cov}}$ as the optimal solution.

### 3.3. Model Solution Results

A search strategy combining equally spaced releases, an optional shared fuse delay, and a two-stage variable-step grid traversal is implemented to obtain the optimal release/detonation schedule and the corresponding trajectories of the three smoke canisters. The temporal distribution of the obscuration period for a single canister is visualized, as illustrated in Fig. 1.

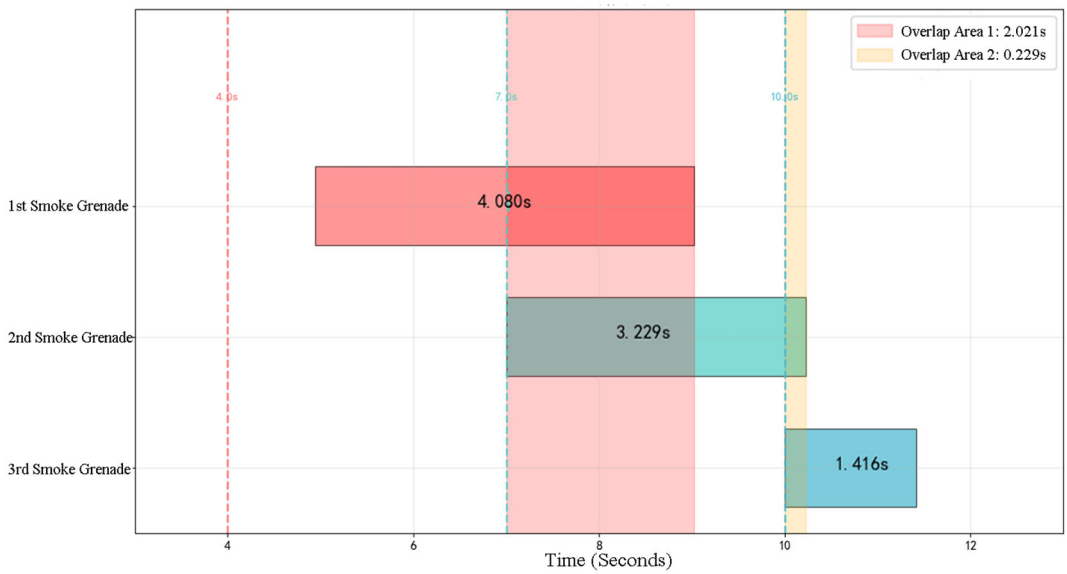


**Fig. 1** Distribution of individual smoke grenade concealment durations

## 4. Multi-Target Robust Obscuration Optimization and PSO-Based Solution

### 4.1. Model Formulation

#### 4.1.1. Modeling Philosophy: Max-Min Robust Fairness Objective

For the multi-target defense scenario against four incoming missiles, the core objective is to maximize the minimum effective full-obscuration duration across all missiles. This ensures robust protection for the target in the most unfavorable direction relative to the missile attacks, and the objective conforms to the Max-Min fairness optimization paradigm [5].

#### 4.1.2. Decision Variables

For each UAV $u$ (each UAV can carry a maximum of 3 smoke canisters, with $k \in \{1,2,3\}$ denoting the canister index), the decision variables are defined as follows:

Continuous variables: Heading angle $\phi_u$, flight speed $v_u$, release time $t_{u,k}$ of the $k$-th canister, and fuse delay $\tau_{u,k}$ of the $k$-th canister;

Discrete variables: Mission assignment $a_{u,k} \in \{1,2,3,4\}$, where $a_{u,k}$ represents the index of the missile that the $k$-th canister of UAV $u$ primarily serves;

Binary activation variables: $y_{u,k} \in \{0,1\}$, where $y_{u,k}=1$ indicates that the $k$-th canister of UAV $u$ is activated, and $y_{u,k}=0$ indicates it is not.

### 4.1.3. Constraints

1. Flight Trajectory Constraints: $\phi_u \in (-\pi,\pi], \quad v_{\min} \le v_u \le v_{\max}$.

2. Bounds and Ordering of Release Times and Fuse Delays: $0 \le t_{u,1} \le t_{u,2} \le t_{u,3} \le T_{\max}$, $0 \le \tau_{u,k} \le \tau_{\max}$.

3. Minimum Release Interval $t_{u,k+1} - t_{u,k} \ge \Delta_{\min}, k \in \{1,2\}$.

4. Canister Payload Limit: $\sum_{k=1}^{3} y_{u,k} \le K_{\max}, \quad y_{u,k} \in \{0,1\}$.

5. Discrete Assignment Constraints: $a_{u,k} \in \{1,2,3,4\}$.

6. Obscuration Criterion and Duration Calculation Constraints: The full obscuration criterion based on the set $\nu$ of 16 discrete vertices of the cylindrical target is adopted. For missile $m$ at time $t$, an obscuration indicator function $\chi_m(t) \in \{0,1\}$ is defined: $\chi_m(t)=1$ if and only if for all $Q \in \nu$, the line-of-sight (LOS) segment $\overline{M_m(t)Q}$ from the missile position $M_m(t)$ to the target point $Q$ intersects at least one effective smoke cloud; otherwise, $\chi_m(t)=0$.

The effective obscuration duration for missile $m$ is defined as:

$$T_m = \int \chi_m(t)dt \approx \Delta t \sum_j \chi_m(t_j) \tag{15}$$

### 4.1.4. Objective Function: Max-Min + Lexicographic Secondary Objectives

The primary objective is to maximize the minimum obscuration duration among the four missiles within the feasible region:

$$\max T_{\min}(X) = \max \min_{m \in \{1,2,3,4\}} T_m(X) \tag{16}$$

To reduce the randomness of the optimal solutions, lexicographic secondary objectives are introduced: among candidate solutions with the same $T_{\min}(X)$, priority is given to maximizing the total obscuration duration $\sum_m T_m$, and minimizing the dispersion of obscuration durations across missiles. An order-preserving scalarization method is adopted to combine the objectives, with the scalarized objective function:

$$J(X) = T_{\min}(X) + \alpha \bar{T}(X) - \beta \sigma_T(X) \tag{17}$$

where the average obscuration duration $\bar{T}(X)$ and the variance of obscuration durations $\sigma_T(X)$ are defined as:

$$\bar{T}(X) = \frac{1}{4}\sum_{m=1}^{4} T_m, \qquad \sigma_T(X) = \mathrm{Var}\left(\{T_m\}_{m=1}^{4}\right) \tag{18}$$

The weighting parameters satisfy $0 < \alpha \ll \beta \ll 1$, ensuring that the primary objective $T_{\min}(X)$ remains dominant in the optimization.

### 4.2. Model Solution (Particle Swarm Optimization)

#### 4.2.1. Particle Encoding and Initialization

Particle Swarm Optimization (PSO) is applied to solve this mixed-variable optimization problem. The continuous and discrete decision variables of the five UAVs are serialized into a high-dimensional particle vector (e.g., a 40-dimensional encoding). The position and velocity of each particle are randomly initialized within the feasible bounds of the corresponding variables [6].

#### 4.2.2. Feasibility Repair Mechanism

Before evaluating the fitness of each particle, a feasibility repair step is executed to ensure all constraints are satisfied:

1. Release times of canisters for each UAV are sorted in ascending order and adjusted to satisfy the minimum release interval $\Delta_{\min}$;

2. Heading angles $\phi_u$ are wrapped to the valid range $(-\pi, \pi]$;

3. All other continuous variables (speed $v_u$, fuse delay $\tau_{u,k}$, etc.) are clipped to their upper and lower bounds.

The time window for obscuration evaluation is determined by the detonation times of all canisters: let $t_0$ be the earliest detonation time and $t_1$ be the latest detonation time of all activated canisters, the evaluation is performed over the interval $[t_0, t_1 + 20]$.

#### 4.2.3. Fitness Function Evaluation

1. Time is discretized with a step size $\Delta t$ over the predefined evaluation time window, generating discrete time points $t_j$;

2. For each $t_j$, the position $M_m(t_j)$ of each missile $m$ and the center position of each active smoke cloud are calculated;

3. The obscuration indicator $\chi_m(t_j)$ is evaluated for each missile $m$ using the criterion of 16-vertex full obscuration and minimum point-to-segment distance $\leq R_s$;

4. The effective obscuration duration $T_m$ for each missile is computed from the indicator values, and the fitness of the particle is calculated using either the primary objective $T_{\min}(X)$ or the scalarized objective $J(X)$.

#### 4.2.4. PSO Iteration and Termination Criteria

Particles are updated using the standard PSO velocity-position update equations. A feasibility repair is immediately performed on the updated particle positions to maintain feasibility.

Upon termination, the global best particle (optimal solution) and its associated performance metrics are output.

#### 4.2.5. Post-Processing of Optimal Solution

The optimal solution obtained from PSO is re-evaluated with a smaller time step $\Delta t$ to improve accuracy. The final result report includes: Release time and detonation time of each activated smoke canister; Effective obscuration intervals for each missile; Total effective obscuration duration for each missile and the overall Max-Min performance metrics. The results are shown in the Table 1.

**Table 1**. Optimal Solution Data Table

| UAV ID | Canister ID | Heading (°) | Speed (m/s) | Drop Time (s) | Fuse Delay (s) |
|---|---|---|---|---|---|
| F1 | B1 | 12.80670645 | 110.8228154 | 4.584011725 | 7.431996208 |
| F1 | B2 | 178.312291 | 114.0964687 | 2.493353447 | 5.094918268 |
| F1 | B3 | 242.2755966 | 110.7988701 | 2.346996261 | 2.039192729 |
| F2 | B1 | 130.6756717 | 121.3612331 | 2.573607266 | 3.850353457 |
| F2 | B2 | 109.1779126 | 95.87944317 | 3.244839743 | 3.032553267 |
| F2 | B3 | 193.4476299 | 110.2625764 | 4.924550105 | 3.947706442 |
| F3 | B1 | 301.6133094 | 120.4913445 | 3.785646835 | 4.397788183 |
| F3 | B2 | 244.4441137 | 96.26711341 | 3.889055113 | 4.916382888 |
| F3 | B3 | 77.59556866 | 99.23311858 | 0.786872673 | 4.180508354 |
| F4 | B1 | 257.8796466 | 103.5865941 | 2.816716317 | 2.789441098 |
| F4 | B2 | 130.0974696 | 115.5064223 | 1.463575119 | 4.831084132 |
| F4 | B3 | 123.0190083 | 109.0587271 | 4.282268273 | 2.093031188 |
| F5 | B1 | 111.2619855 | 100.390686 | 5.081566475 | 7.264294176 |
| F5 | B2 | 318.2458734 | 96.84045537 | 3.50916353 | 5.669697975 |
| F5 | B3 | 71.70794025 | 106.5080437 | 4.813136927 | 4.673416022 |

## 5. Conclusion

This paper proposes an engineering-feasible collaborative optimization framework for smoke-screen concealment under multiple incoming missiles. The target is discretized into 16 representative points, and a minimum-distance criterion between line-of-sight segments and spherical smoke clouds is used to evaluate obscuration effectiveness. Multiple smoke clouds are modeled as their union, and time discretization with boundary refinement is applied to accumulate the effective concealment duration. To address multi-target protection requirements, a Max-Min robust fairness objective is introduced. Particle swarm optimization is employed to search approximately 40 mixed decision variables, with a feasibility repair mechanism to satisfy constraints. Future research may further consider wind disturbances.

## References

[1] Si Pengbo, Wu Bing, Yang Ruizhe, et al. Path Planning for Unmanned Aerial Vehicles Based on Multi-Agent Deep Reinforcement Learning [J]. Journal of Beijing University of Technology, 2023, 49(04): 449-458.

[2] Tian Xuetao, Xi Qingbiao. Real-Time Trajectory Planning for UAVs Based on Mixed-Integer Linear Programming [J]. Computer Simulation, 2009, 26(05): 72-75.

[3] Liu Liu, Zhang Liqiang, Zhang Liang, et al. Line-of-Sight Analysis for Complex Terrain Scenarios Based on an Improved LOS Algorithm [J]. Science China: Information Sciences, 2011, 41(06): 675-685.

[4] Feng Qian, Li Qing, Quan Wei, et al. Research Review on Multi-Objective Particle Swarm Optimization Algorithms [J]. Journal of Engineering Sciences, 2021, 43(06): 745-753. DOI:10.13374/j.issn2095-9389.2020.10.31.001.

[5] Huang, Y. J., Jin, Y. C., & Hao, K. R. Time-domain robust optimization algorithm for constrained problems based on swarm intelligence. Control and Decision, 2020, 35(03): 740-748. DOI:10.13195/j.kzyjc.2018.0591.

[6] Shi Cuicui, Liu Yuanhua, Chen Xin. Water Quality Prediction Model Based on Particle Swarm Optimization of Support Vector Regression [J]. Information and Control, 2022, 51(03): 307-317. DOI: 10.13976/j.cnki.xk.2022.1125.